

## Molecular ions of 3,3'-bi(2-R-5,5-dimethyl-4-oxopyrrolinylidene) 1,1'-dioxides

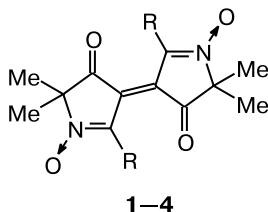
L. A. Shundrin,\* I. G. Irtegova, A. D. Rogachev, and V. A. Reznikov

N. N. Vorozhtsov Institute of Organic Chemistry, Siberian Branch of the Russian Academy of Sciences,  
9 prosp. Akad. Lavrent'eva, 630090 Novosibirsk, Russian Federation.  
Fax: +7 (383) 330 9752. E-mail: Leonid.Shundrin@niboch.nsc.ru

The electrochemical reduction of 3,3'-bi(2-R-5,5-dimethyl-4-oxopyrrolinylidene) 1,1'-dioxides (R = CF<sub>3</sub>, Me, Ph, Bu<sup>t</sup>), which are cyclic dinitrons with conjugated C=C bond, in acetonitrile is an EE process producing stable radical anions and dianions, whereas the electrochemical oxidation is an EEC (R = Me, Ph) or EE process (R = Bu<sup>t</sup>) with formation of radical cations (except for the case of R = CF<sub>3</sub>) and dications (R = Bu<sup>t</sup>) stable under standard conditions. Radical cations of the dioxides with R = Me, Ph, and Bu<sup>t</sup> and radical anions of the whole series of the compounds studied, including R = CF<sub>3</sub>, were characterized by ESR spectroscopy combined with electrochemical measurements and quantum-chemical calculations. The electrochemical behavior of the Bu<sup>t</sup>-substituted dinitron is unique: the EE processes in the region of negative and positive potentials with formation of the dianion, radical anion, radical cation, and dication stable at *T* = 298 K were observed for the first time within one cycle of potential sweep in the CV curve measured in MeCN.

**Key words:** 3,3'-bi(2-R-5,5-dimethyl-4-oxopyrrolinylidene) 1,1'-dioxides, cyclic nitrons, electroreduction, electrooxidation, cyclic voltammetry, radical anions, dianions, radical cations, dications, ESR spectroscopy.

It has previously<sup>1</sup> been shown that 3,3'-bi(2-R-5,5-dimethyl-4-oxopyrrolinylidene) 1,1'-dioxides **1–4**, being cyclic dinitrons with conjugated C=C bond, have a considerable electron-withdrawing ability comparable with that of tetracyanoethylene,<sup>2</sup> and their electrochemical reduction (ECR) in DMF is an EE process (includes two one-electron electrochemical steps) with formation of radical anions (RA) and dianions (DA) stable at *T* = 298 K.

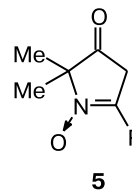


R = CF<sub>3</sub> (**1**), Me (**2**), Ph (**3**), Bu<sup>t</sup> (**4**)

The one-electron reduction of dinitrons **1–4** is accompanied by the formation of the corresponding RA detected in the ESR spectra. According to these data, in the radical-anion states, the substituents in positions 2 of the pyrrolinone rings disturb weakly the  $\pi$ -system  $O \leftarrow N=C-C=C-C=N \rightarrow O$ , both <sup>14</sup>N nuclei are spectrally equivalent, the corresponding isotropic hyperfine interaction (IHFI) constants *a<sub>N</sub>* are close in magnitude and vary in a range of  $\pm 0.004$  mT with R variation, and

hyperfine coupling with the substituent nuclei appears only in the cases of R = CF<sub>3</sub> and Me.

Dinitrons **1–4** are formed due to the mild chemical oxidation of the starting pyrrolinones **5**.<sup>3</sup> The extension of the  $\pi$ -system in compounds **1–4** compared to the starting pyrrolinones should decrease an energy gap between the levels of the frontier MOs ( $\Delta\epsilon = \epsilon_{\text{LUMO}} - \epsilon_{\text{HOMO}}$ , LUMO and HOMO are the lowest unoccupied and highest occupied MOs, respectively) and result in an easier one-electron oxidation and, probably, stabilization of the positively charged molecular ions (*cf.* Ref. 4). To study a possibility of formation and estimate stability limits of radical cations (RC) and dications (DC), we studied the electrochemical oxidation (ECO) and, for comparison, ECR of compounds **1–4** in MeCN by cyclic voltammetry (CV) and ESR spectroscopy.



R = CF<sub>3</sub>, Me, Ph, Bu<sup>t</sup>

### Experimental

Cyclic voltammograms of dinitrons **1–4** were measured on an SVA-1BM electrochemical system (Bulgaria) equipped with a LAB-MASTER polyfunctional interface (Institute of Nuclear Physics, Novosibirsk, Russia), which enables one complete digi-

tal control of the system. Measurements were carried out in a mode of triangular pulse potential sweep in the range of sweep rates  $0.1 \text{ V s}^{-1} < \nu < 50 \text{ V s}^{-1}$ . A standard electrochemical cell with a working volume of 5 mL switched to the system *via* the three-electrode scheme and equipped with a salt bridge filling with a supporting electrolyte solution in MeCN to connect the working volume and reference electrode. The working electrode was a stationary spherical Pt electrode with a surface area of  $8 \text{ mm}^2$ , a Pt spiral was the auxiliary electrode, and a saturated aqueous calomel electrode (SCE) served as the reference electrode. The supporting electrolyte was  $\text{Et}_4\text{NClO}_4$  ( $0.1 \text{ mol L}^{-1}$ ). Oxygen was removed by passing argon through the working solution. The concentration of depolarizers was  $1 \cdot 10^{-3} \text{ mol L}^{-1}$ .

ESR spectra of paramagnetic intermediates of the ECO and ECR processes were measured on a Bruker ESP-300 radio-spectrometer equipped with a double resonator. Compounds **1–4** were oxidized and reduced in combination with ESR spectrometric measurements under anaerobic conditions at potentials of the corresponding oxidation or reduction peaks at  $T = 298 \text{ K}$  in a three-electrode cell with a Pt electrode. The space of the working electrode of the cell was placed into the front shoulder of the ESR spectrometer resonator. Numerical simulation of ESR spectra were performed according to the Winsim 32 program with the LMB1 multiparametric optimization algorithm.

To establish possible structures and energies of the frontier orbitals of compounds **1–4**, as well as those of their RC and DC, quantum-chemical calculations of the corresponding species were carried out by the unrestricted (UHF) and restricted Hartree–Fock (RHF) methods in the PM3 approximation. The calculations were performed by the WinMOPAC 7.0 and Hyperchem 7.0 programs with complete geometry optimization and symmetry restraints for the Me groups in position 5 of the pyrrolinone cycles and for substituents in position 2 according to their local dynamic symmetry ( $C_{3v}$  for the  $\text{CF}_3$ , Me, and  $\text{Bu}^t$  groups and  $C_{2v}$  for Ph). No restraints were imposed on rotation of all substituents about the pyrrolinone cycles.

## Results and Discussion

The cyclic voltammograms of compounds **1–4** in the region of negative potentials contain two reversible one-electron reduction peaks corresponding to the formation of RA and DA stable in MeCN at  $T = 298 \text{ K}$ , *i.e.*, the replacement of the DMF solvent by MeCN does not qualitatively change the reduction processes. In MeCN, the potentials of reduction peaks are by approximately  $0.1 \text{ V}$  shifted to the region of more negative values compared to the potentials measured in DMF.<sup>1</sup>

The CV curves of compounds **1–4** in the region of positive potentials are shown in Fig. 1. For the potential sweep rate  $\nu < 5 \text{ V s}^{-1}$ , the CV curve of **1** exhibits the single irreversible oxidation peak. It is most likely that the irreversibility is caused by a fast chemical reaction involving RC. In turn, the ECO of dinitrons **2** and **4** is characterized by two peaks, whereas four oxidation peaks are observed for **3**. The observed peaks are characterized hereinafter by potentials in the region of positive ( $E_{(+)ij}$ ) and

negative ( $E_{(-)ij}$ ) values, respectively ( $i$  is the number of peak, and  $j = a$  or  $c$  indicates the anodic or cathodic branch, respectively, of the CV curve). The first oxidation peaks of all compounds are diffuse in nature,  $I_{(+)1a\nu^{0.5}} = \text{const}$ , where  $I_{(+)1a}$  is the maximum current of the first peak in the anodic branch of the voltammogram.\* For compounds **2–4**, the first peaks correspond to the reversible one-electron process (ratio of currents of the anodic and cathodic branches  $I_{(+)1a}/I_{(-)1c} \approx 1$  and  $\Delta E = E_{(+)1a} - E_{(-)1c} = 0.06 \text{ V}$ ).

At low sweep rates ( $\nu < 4 \text{ V s}^{-1}$ ), the second oxidation peak of **2** is irreversible, and in the range  $5 \text{ V s}^{-1} < \nu < 50 \text{ V s}^{-1}$  the voltammogram of **2** exhibits two reversible one-electron peaks (see Fig. 1, *b*). Noticeable instability of DC of **2** formed at the potential of the second oxidation peak is related, most likely, to proton elimination from the methyl group in position 2 (see also Ref. 5). In fact, when the methyl groups are replaced by the *tert*-butyl groups, the ECO of dinitron **4** in MeCN at  $T = 298 \text{ K}$  is an EE process with formation of stable RC and DC in the whole studied range of  $\nu$  (see Fig. 1, *d*).

The peak corresponding to the formation of DC **3** is irreversible ( $E_{(+)2a}$ ,  $\nu < 5 \text{ V s}^{-1}$ , see Fig. 1, *c*), the ratio is  $I_{(+)2a}/I_{(+)1a} = 2.57$ , and two additional oxidation peaks, whose nature was not studied, are observed in the anodic branch. As in the case of methyl-substituted dinitron **2**, when  $\nu$  is increased to  $5 \text{ V s}^{-1}$ , the  $E_{(+)2a}$  peak becomes reversible and one-electron in height ( $I_{(+)2a}/I_{(+)1a} = 0.97$ ), and the  $E_{(+)4a}$  peak observed at low potential sweep rates disappears (see Fig. 1, *c*, lower curve). The irreversible (at all  $\nu$ ) peak  $E_{(+)5c}$  in the cathodic branch of the voltammogram is attributed, most likely, to the ECO of the conversion products of DC **3**, because this peak is not observed for the potential sweep in an interval of  $0 \text{ V} < E < 1.7 \text{ V}$ .

To establish the nature of the oxidation peak of trifluoromethyl-substituted dinitron derivative **1**, we measured the CV curves in the potential sweep region  $-1.0 \text{ V} < E < 2.2 \text{ V}$  (Fig. 2, *a*) and in the rate range  $0.1 \text{ V s}^{-1} < \nu < 50 \text{ V s}^{-1}$ . For  $\nu = 0.1 \text{ V s}^{-1}$ , the ratio of absolute values of currents of the observed oxidation peak and reversible one-electron reduction peak is  $|I_{(+)1a}|/|I_{(-)1c}| = 2.7$ . In an interval of  $0.1 \text{ V s}^{-1} < \nu < 10 \text{ V s}^{-1}$ , the ratio decreases exponentially to 1.26 and remains constant up to  $\nu = 50 \text{ V s}^{-1}$  (Fig. 3). The plots of currents of the oxidation peak of dinitron **1** and its first reduction peak corresponding to the formation of RA **1** vs. potential sweep rate are shown in Fig. 3 along with similar plots for *tert*-butyl-substituted dinitron **4**, whose all one-electron peaks are reversible in both the negative and positive potential regions (see Fig. 2, *b*). The dependences of all currents of the reversible peaks on the po-

\* The principle of designation of peak currents is the same as that for the corresponding potentials.

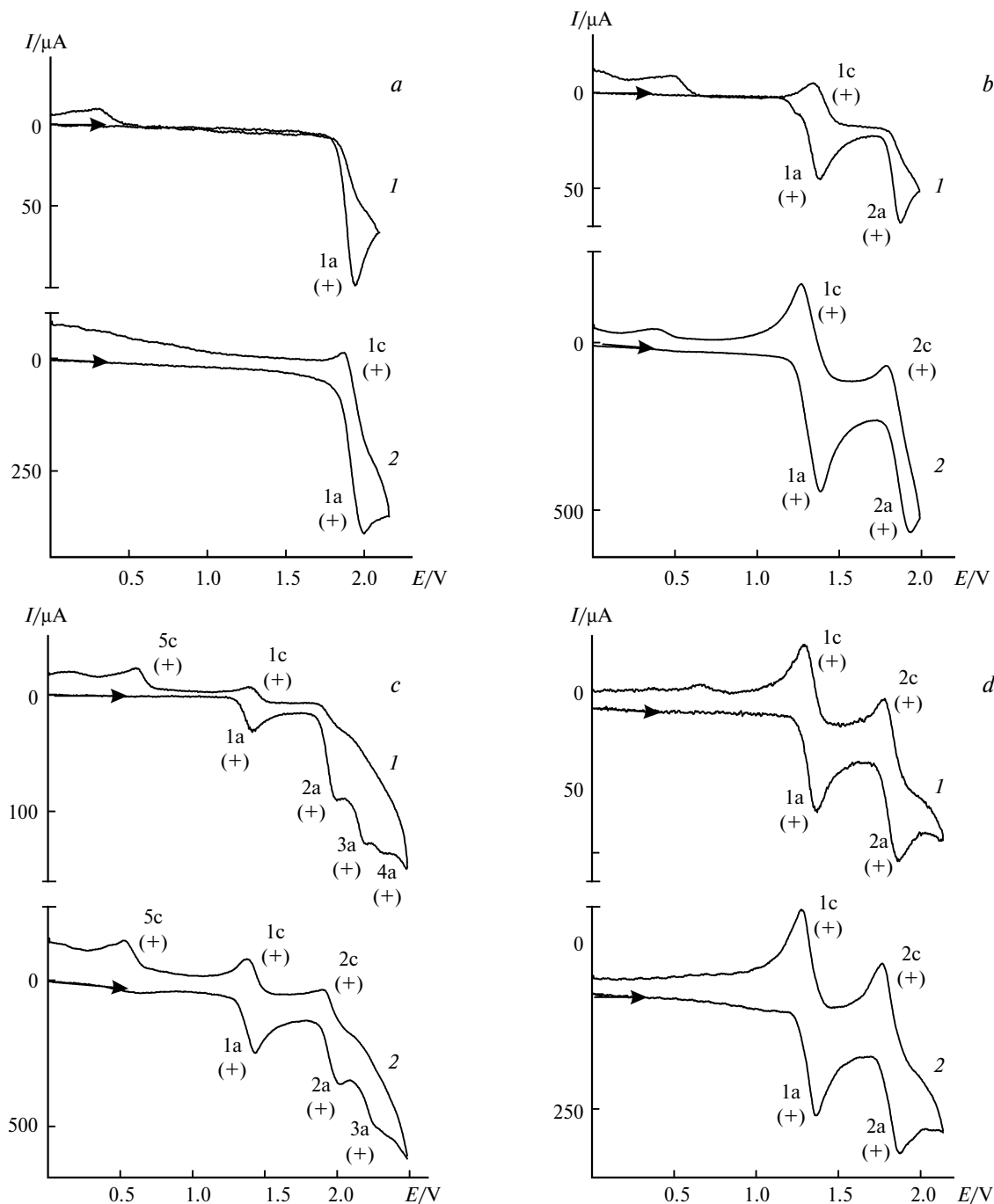


**Fig. 1.** Cyclic voltammograms of dinitrons **1–4** (*a–d*, respectively) in the region of positive sweep potentials and  $\nu = 0.1$  (*I*),  $5.0 \text{ V s}^{-1}$  (*2*);  $C_0 = 1 \cdot 10^{-3} \text{ mol L}^{-1}$ , MeCN, supporting electrolyte  $0.1 \text{ M Et}_4\text{NClO}_4$ .

tential sweep rate are well described by the classical equation

$$I_{(\pm)}^{\ddot{}} = B + A\nu^{0.5}, \quad (1)$$

where  $A = nFS_{\text{el}}D^{0.5}C_0$ ,  $n = 1$  is the number of transferred electrons,  $S_{\text{el}}$  is the surface area of the working electrode,  $D$  is the diffusion coefficient of the substance,  $C_0$  is the

depolarizer concentration, and  $B$  is an empirical constant related to the perturbation of linear free diffusion. The parameters in Eq. (1)  $A$ ,  $B$ , and  $r^2$  ( $r^2$  is the correlation coefficient) have the following values: dinitron **1**,  $I_{(-)}^{1c}$ ,  $-67.56 \text{ } \mu\text{A V}^{-0.5} \text{ s}^{0.5}$ ,  $7.73 \text{ } \mu\text{A}$ , and  $0.998$ ; dinitron **4**,  $I_{(-)}^{1c}$ ,  $-65.95 \text{ } \mu\text{A V}^{-0.5} \text{ s}^{0.5}$ ,  $-0.33 \text{ } \mu\text{A}$ ,  $0.997$ ,  $I_{(+)}^{1a}$ ,  $88.88 \text{ } \mu\text{A V}^{-0.5} \text{ s}^{0.5}$ ,  $4.41 \text{ } \mu\text{A}$ , and  $0.998$ .

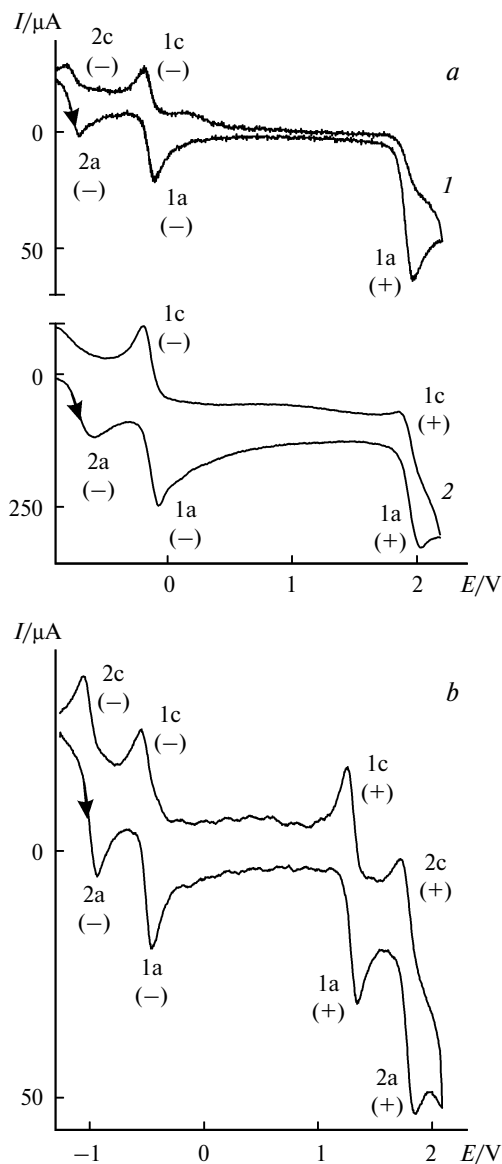


**Fig. 2.** Cyclic voltammograms of dinitrons **1** (*a*,  $\nu = 0.1$  (1) and  $5 \text{ V s}^{-1}$  (2)) and **4** (*b*,  $\nu = 0.1 \text{ V s}^{-1}$ );  $C_0 = 1 \cdot 10^{-3} \text{ mol L}^{-1}$ , MeCN, supporting electrolyte  $0.1 \text{ M Et}_4\text{NClO}_4$ .

The dependence of the oxidation peak current of **1** on the potential sweep rate is described by the equation

$$I_{(+)}^{1a} = B + A\nu^{0.5} + C\exp(-k\nu^{0.5}), \quad (2)$$

where  $C$  and  $k$  are empirical constants. The parameters in Eq. (2) for  $I_{(+)}^{1a}$  are the following:  $A = 88.33 \mu\text{A V}^{-0.5} \text{ s}^{0.5}$ ,  $B = 6.28 \mu\text{A}$ ,  $C = 35.33 \mu\text{A}$ ,  $k = 1.48 \text{ V}^{-0.5} \text{ s}^{0.5}$ , and  $r^2 = 0.996$ . The last term in Eq. (2) reflects the contribution of the electrodic process associated with the oxidation of the conversion products of RC **1**. This process seems to be rather slow in the CV time scale. Hence, for a relatively low increase in  $\nu$  (up to  $5 \text{ V s}^{-1}$ ), Eq. (2) can rapidly be reduced to Eq. (1), the oxidation peak of **1**

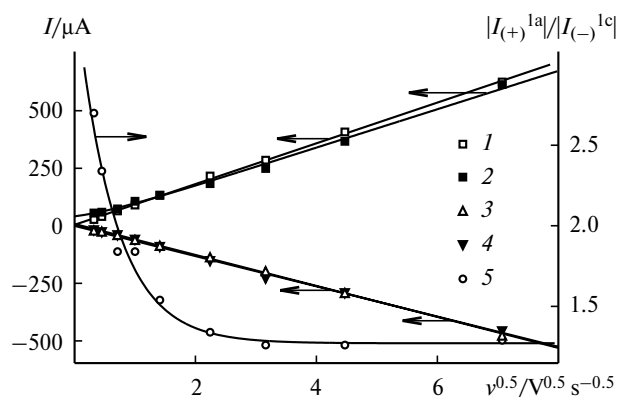


**Fig. 3.** Currents of the first oxidation ( $I_{(+)}^{1a}$ ) and reduction ( $I_{(-)}^{1c}$ ) peaks of dinitrons **1** (1, 3) and **4** (2, 4) and the ratio  $|I_{(+)}^{1a}|/|I_{(-)}^{1c}|$  (5) for dinitron **1** vs.  $\nu^{0.5}$ .

becomes reversible and one-electron in height, and the slope ( $A$ ) of the plot of the peak current vs.  $\nu^{0.5}$  is virtually equal to that of  $I_{(+)}^{1a}(\nu^{0.5})$  for **4** (see Fig. 3). In the region of negative potentials, the slopes of the plots of the currents of the first reduction peaks of **1** and **4** ( $I_{(-)}^{1c}$ ) are fairly close (see Fig. 3).

Thus, the first step of oxidation of compounds **1–4** in MeCN is the one-electron transfer to form RC **1–4**. For trifluoromethyl-substituted dinitron **1**, the observed current of the first oxidation peak at low  $\nu$  contains a contribution from the electrode process related to the oxidation of the conversion products of RC **1**. A similar situation is observed for the second step of oxidation of **3**. The second ECO step of dinitrons **2** and **4** is one-electron but only DC **4** is noticeably stable. Note that both ECO and ECR of *tert*-butyl-substituted dinitron **4** are EE processes accompanied by the formation of DA, RA, RC, and DC stable at  $T = 298 \text{ K}$  (see Fig. 2, *b*). Perhaps, this is the first example of an organic heterocyclic compound for which four stable molecular ions were detected within one potential sweep cycle.

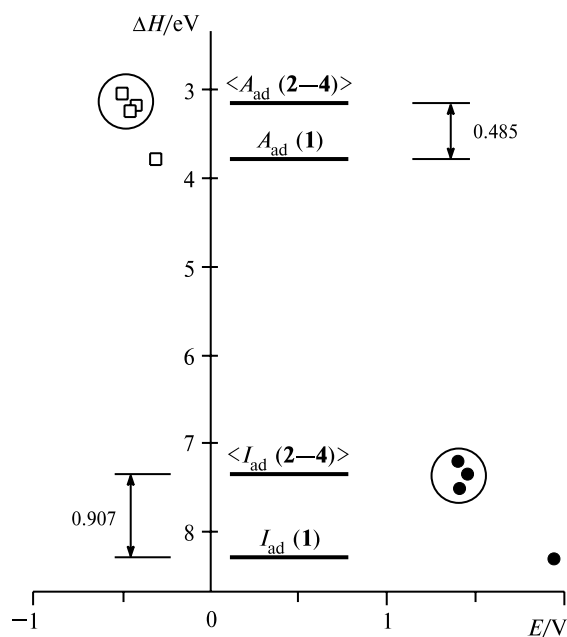
The potentials of the first two ECO and ECR peaks of **1–4** measured in MeCN are presented in Table 1. The potentials of the first peaks of both ECO and ECR of dinitrons **2–4** are close in absolute value, and the introduction of the trifluoromethyl group into position 2 shifts noticeably both potentials toward more positive and less negative potentials, respectively. Figure 4 shows the correspondence between the experimentally observed potentials of the first ECO and ECR peaks of **1–4**, adiabatic ionization potentials, and adiabatic electron affinities calculated by the RHF(UHF)/PM3 methods and determined as  $I_{ad} = E_{RC}^{UHF} - E_n^{RHF}$  and  $A_{ad} = E_n^{RHF} - E_{RA}^{UHF}$ , where  $E_n^{RHF}$ ,  $E_{RA}^{UHF}$ , and  $E_{RC}^{UHF}$  are the full energies of the neutral species of **1–4** and their RA and RC in the optimized conformations calculated in the corresponding approximations of the Hartree–Fock method. For dinitrons **2–4**, the ECO and ECR potentials and calculated

**Table 1.** Potentials of the ECO and ECR<sup>a</sup> peaks ( $E$ ), adiabatic ionization potentials ( $I_{\text{ad}}$ ), and adiabatic electron affinity ( $A_{\text{ad}}$ ) of compounds **1–4** calculated by the Hartree–Fock method in the PM3 approximation

Com- pound	R	Oxidation <sup>b</sup>					Reduction				
		$E_{(+)}^{1a}$	$E_{(+)}^{1c}$	$E_{(+)}^{2a}$	$E_{(+)}^{2c}$	$I_{\text{ad}}$	$-E_{(-)}^{1c}$	$-E_{(-)}^{1a}$	$-E_{(-)}^{2c}$	$-E_{(-)}^{2a}$	$A_{\text{ad}}$
		V					V				
<b>1</b>	CF <sub>3</sub>	1.94 (1.98)	— (1.88)	—	—	8.21	0.81	0.71	0.18	0.11	3.688
<b>2</b>	Me	1.38 (1.39)	1.32 (1.30)	1.88 (1.90)	— (1.80)	7.50	1.07	1.00	0.58	0.48	3.103
<b>3</b>	Ph	1.41 (1.41)	1.36 (1.35)	1.98 (2.00)	— (1.89)	7.11	1.05	0.95	0.55	0.47	3.243
<b>4</b>	Bu <sup>t</sup>	1.36 (1.36)	1.29 (1.26)	1.86 (1.87)	1.78 (1.77)	7.30	1.00	0.93	0.52	0.45	3.263

<sup>a</sup> At the Pt electrode vs. SCE in an 0.1 M solution of Et<sub>4</sub>NClO<sub>4</sub> in MeCN,  $C_0 = 1 \cdot 10^{-3}$  mol L<sup>-1</sup>, potential sweep rate 0.1 V s<sup>-1</sup>.

<sup>b</sup> Peak potentials at a potential sweep rate of 5 V s<sup>-1</sup> are given in parentheses.

**Fig. 4.** Correspondence of the PM3-calculated adiabatic electron affinity ( $A_{\text{ad}}$ ) and adiabatic ionization potentials ( $I_{\text{ad}}$ ) of dinitrons **1–4** to the potentials of the first peaks of their ECR and ECO.

$I_{\text{ad}}$  and  $A_{\text{ad}}$  values are close, and their averaged  $\langle I_{\text{ad}} \rangle$  and  $\langle A_{\text{ad}} \rangle$  values are equal to 7.303 and 3.203 eV, respectively (see Fig. 4). The introduction of the electron-withdrawing CF<sub>3</sub> group into position 2 of the cycle (dinitron **1**) increases  $A_{\text{ad}}$  and  $I_{\text{ad}}$  by 0.485 and 0.907 eV, respectively. In the case of both one-electron oxidation and one-electron reduction, the  $\pi$ -system of dinitrons **1–4** is rather conservative to the effect of a substituent in position 2, while the introduction of a sufficiently strong electron-

**Table 2.** Comparative characteristics of the ESR spectra<sup>a</sup> of RA and RC **1–4** generated in MeCN at 298 K

Com- pound	R	IHF constants/mT	
		RA	RC
<b>1</b>	CF <sub>3</sub>	0.462 ( <sup>14</sup> N), 0.217 ( <sup>19</sup> F)	
<b>2</b>	Me	0.414 ( <sup>14</sup> N), 0.173 ( <sup>1</sup> H)	0.141 ( <sup>14</sup> N), 0.083 ( <sup>1</sup> H) <sup>b</sup>
<b>3</b>	Ph	0.425 ( <sup>14</sup> N)	0.150 ( <sup>14</sup> N)
<b>4</b>	Bu <sup>t</sup>	0.435 ( <sup>14</sup> N)	0.188 ( <sup>14</sup> N)

<sup>a</sup> The radical anions were generated in MeCN at the corresponding potentials of the first reduction peak  $E_{(-)}^{1c}$ , and the radical cations were generated at the potential  $E_{(+)}^{1a}$ ; the concentration of the depolarizer and Et<sub>4</sub>NClO<sub>4</sub> was  $1.5 \cdot 10^{-3}$  and 0.1 mol L<sup>-1</sup>, respectively.

<sup>b</sup> The hyperfine structure 5N×7H becomes resolved at  $T < 253$  K.

withdrawing substituent (CF<sub>3</sub> group) does not change the type of the frontier MOs.

Under the ECR conditions for compounds **1–4**, the ESR spectra of the corresponding RA are detected at potentials of the first cathodic peaks ( $E_{(-)}^{1c}$ ) (Fig. 5), and their characteristics are presented in Table 2. The character of the hyperfine structure of the ESR spectra of all RA generated in MeCN is the same as that for RA in DMF.<sup>1</sup> Only a slight increase in the IHFI constants with the <sup>14</sup>N nuclei is observed compared to the corresponding constants for RA in DMF. For RA **1** and **2**, all <sup>19</sup>F and <sup>1</sup>H nuclei of R substituents are spectrally equivalent and give septet hyperfine splitting with the binominal ratio of intensities of the components. At  $T = 298$  K, no dynamic effects are observed, which are related to inhibited rotation of the substituents in position 2 or torsional oscillations of the pyrrolinone moieties about the C=C bond when the solvent is replaced.

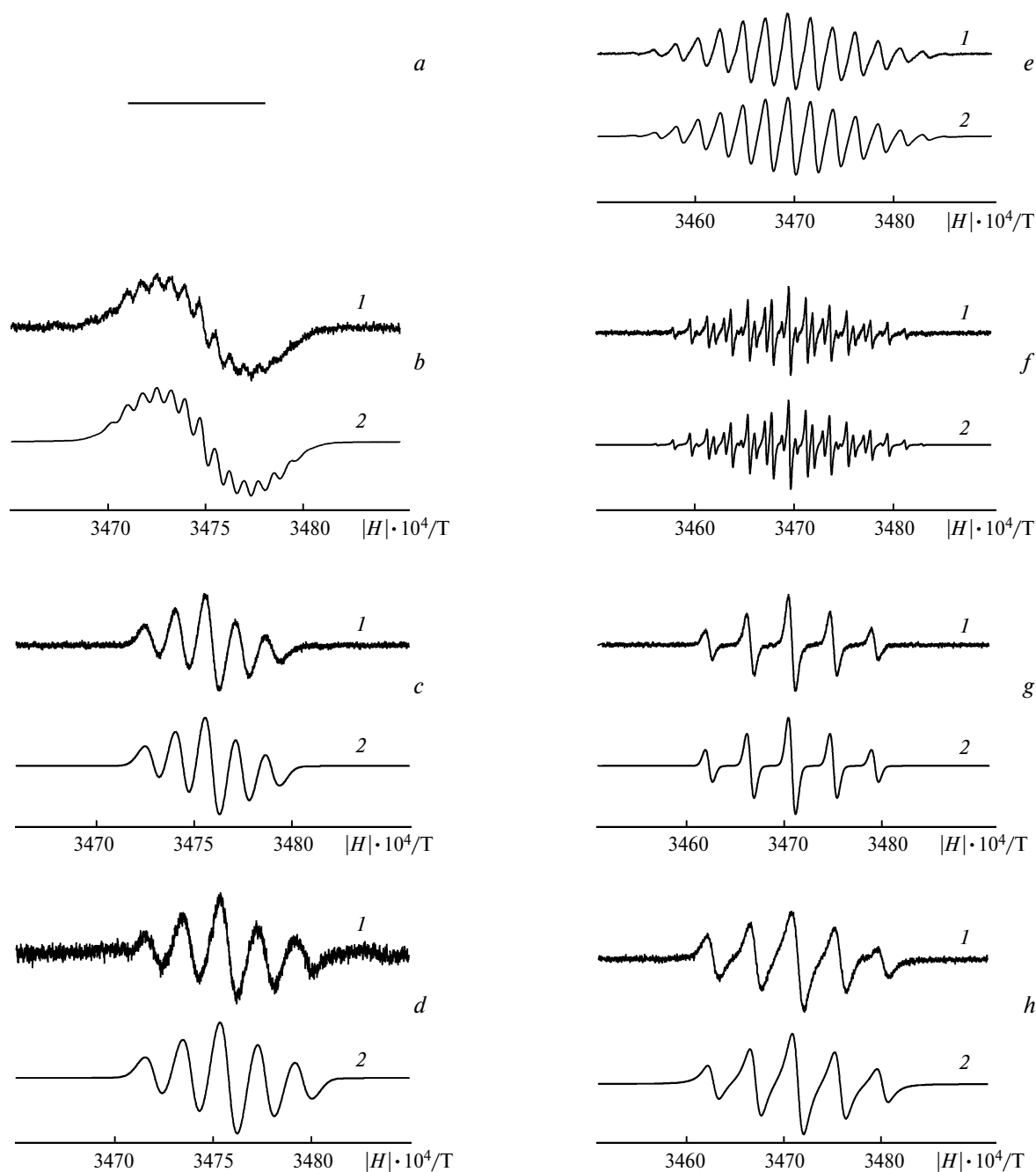


**Fig. 5.** ESR spectra of (1) RC (a–d) and RA (e–h) of dinitrons **1** (a, e), **2** (b, f), **3** (c, g), and **4** (d, h) generated by electrochemical oxidation and reduction in MeCN (298 K) at the corresponding potentials of the first peaks and their mathematical reconstructions (2).

For the ECO of dinitrons **2–4**, the ESR spectra of the corresponding RC are observed at potentials of the first anodic peaks  $E_{(+)}^{1a}$  (see Fig. 5). The nitrogen atoms of all RC are spectrally equivalent. A rather resolved hyperfine structure from protons of the substituents in position 2 of the pyrrolinone cycles is observed only for RC of methyl dinitron derivative **2** at  $T = 253$  K, and the ESR spectra of RC **1** were not detected because of its instability (see

Fig. 1, a). The IHFI constants for RC **2–4** are presented in Table 2.

On going from RA to the corresponding RC **2–4**, the experimentally observed nitrogen hyperfine splitting constant decreases, on the average, by 2.69 times (see Table 2), and the IHFI constants with the  $^1\text{H}$  nuclei of the methyl groups (pair of RA **2**, RC **2**) decrease by 2.08 times. No IHFI constants with protons of the

**Table 3.** Dihedral angles ( $\theta$ /deg) between the pyrrolinone cycles in dinitrons **1–4** and their molecular ions according to the data of X-ray diffraction<sup>7</sup> and PM3 calculations in the UHF and RHF approximations

Compound	R	$\theta_{\text{XRD}}$	$\theta_n$		$\theta_{\text{RC}}$		$\theta_{\text{DC}}$		$\theta_{\text{RA}}$		$\theta_{\text{DA}}$	
			UHF	RHF	UHF	RHF	UHF	RHF	UHF	RHF	UHF	RHF
<b>1</b>	CF <sub>3</sub>	—	44.2	30.8	47.6	47.6	—	—	45.9	47.7	89.8	89.8
<b>2</b>	Me	32.0	38.2	30.1	36.6	36.7	39.3	42.7	37.0	37.4	41.4	43.9
<b>3</b>	Ph	47.6	63.6	37.2	47.8	48.7	58.2	73.9	67.7	56.0	86.6	80.6
<b>4</b>	Bu <sup>†</sup>	51.5	—*	55.1	88.0	72.1	86.9	86.9	62.7	72.7	—*	—*

\* No results are given, because the calculated geometry is not stationary in the BFGS optimization.

*tert*-butyl and phenyl groups are observed for both RA and RC **3** and **4**.

The PM3 calculations of the geometric parameters of the neutral species and molecular ions of **1–4** in the ground state show that all structures have the  $C_2$  symmetry. In the molecular ions, both pyrrolinone cycles are planar in fact, and the angle between the cycles ( $\theta$ ) increases with an increase in the effective volume of substituent R (Table 3), whereas the  $\theta$  values are higher than those for the neutral species and increase with an increase in the ion charge.

According to the UHF/PM3 calculations for both types of paramagnetic ions **2–4**, the  $^{14}\text{N}$  nuclei in the pyrrolinone cycles should be spectrally equivalent, which is confirmed by experiment. The corresponding spin site occupancies of the 2s-AOs of the nitrogen atoms are the following: ( $S_{2s\text{-AO}}(\text{RA } \mathbf{2})$ ,  $S_{2s\text{-AO}}(\text{RC } \mathbf{2})$ ) = (0.02166, –0.00181); ( $S_{2s\text{-AO}}(\text{RA } \mathbf{3})$ ,  $S_{2s\text{-AO}}(\text{RC } \mathbf{3})$ ) = (0.02354, –0.00196); ( $S_{2s\text{-AO}}(\text{RA } \mathbf{4})$ , and  $S_{2s\text{-AO}}(\text{RC } \mathbf{4})$ ) = (0.02314, –0.00125). Therefore, the calculation predicts qualitatively the close constants in the series of RC **2–4** and RA **2–4** and a considerable decrease in the  $a_N$  constant on going from RA to RC. At the same time, the UHF/PM3 method significantly overestimates the spin site occupancies of the 1s-AOs of the H atoms in the benzene rings of RA **3**. The calculation of the spin density of RA and RC **3** by the UHF/INDO variant using the geometry optimized by the UHF/PM3 method<sup>6</sup> is more adequate to the experimental data. On going from RA **3** to its RC, the spin density shifts, to a great extent, to the O atoms bonded to the N atoms, which should decrease the IHFI constants with the  $^{14}\text{N}$  nuclei and spin density on the C atoms in position 2 of the cycles. For RA and RC **2** and **4**, the calculation gives a similar result, which is qualitatively confirmed by measurements of the ESR spectra of the corresponding species (see Table 2).

The data of ESR spectroscopy combined with the results of quantum-chemical calculations show that RA **1–4** and RC **2–4** are  $\pi$ -radicals with the spin-polarization mechanism of IHFI with the  $^{14}\text{N}$  nuclei. According to the quantum-chemical calculations, the arrangement of the pyrrolinone cycles in the equilibrium conformation is non-coplanar, and the singly occupied MO in both types of molecular ions is delocalized over the system of bonds  $\text{O} \leftarrow \text{N}=\text{C}-\text{C}=\text{C}-\text{C}=\text{N} \rightarrow \text{O}$  and carbonyl group.

Thus, generalizing the results of our study and earlier published data,<sup>1,3,7</sup> one can assert that we described the electrochemical behavior of the new class of heterocyclic compounds of the nitron series with a very high electron-withdrawing ability capable of forming molecular ions stable in aprotic media.

## References

1. L. A. Shundrin, V. A. Reznikov, I. G. Irtseva, and V. F. Starichenko, *Izv. Akad. Nauk, Ser. Khim.*, 2003, 892 [*Russ. Chem. Bull., Int. Ed.*, 2003, **52**, 939].
2. Ch. K. Mann and K. K. Barnes, *Electrochemical Reactions in Nonaqueous Systems*, Marcel Dekker, New York, 1970.
3. V. A. Reznikov, V. V. Martin, and L. B. Volodarskii, *Izv. Akad. Nauk SSSR, Ser. Khim.*, 1990, 1398 [*Bull. Acad. Sci. USSR, Div. Chem. Sci.*, 1990, **39**, 1261 (Engl. Transl.)].
4. H. Miyazaki, Y. Matsuhisa, and T. Kubota, *Bull. Chem. Soc. Jpn.*, 1981, **54**, 3850.
5. A. S. Morkovnik and O. Yu. Okhlobystin, *Khim. Geterotsikl. Soedin.*, 1980, 1011 [*Chem. Heterocycl. Compd.*, 1980, No. 8 (Engl. Transl.)].
6. T. Clark, *A Handbook of Computational Chemistry*, Wiley-Interscience, New York, 1985, 352 pp.
7. T. V. Rybalova, Yu. V. Gatilov, V. A. Reznikov, N. V. Pervukhina, and A. B. Burdukov, *Zh. Strukt. Khim.*, 1997, **38**, 775 [*Russ. J. Struct. Chem.*, 1997, **38**, 648 (Engl. Transl.)].

Received July 20, 2004;  
in revised form November 17, 2004